EUROPEAN ORGANIZATION FOR NUCLEAR RESEARCH

DIRAC Note 2006-02
June 5, 2006

Evaluation of the measurement of multiple scattering for the DIRAC set-up, using standard DIRAC analysis tools

A.Benelli, D. Drijard, O.Gorchakov, L.Tauscher, V.Yazkov

GENEVA
2006

1 Introduction

The aim of the study is to evaluate a dedicated measurement of multiple scattering done in 2003 for materials, that are crossed by particles detected by the DIRAC set-up. For this purpose we use standard DIRAC ARIANE procedures, in contrast to the precision analysis by Kruglov [2], which made use of special alignment procedures. For comparison, Monte Carlo simulations were done using the multiple scattering algorithm found by [2], henceforth called "DIRAC-ms", and standard (GEANT) Moliere modified multiple scattering, henceforth called "Moliere-ms". While "DIRAC-ms" uses the directly measured distributions as reconstructed in [2], "Moliere-ms" uses the material budgets from the detector descriptions in DIRAC-GEANT.

The materials were: Ni (target thickness 94μm), Al-window at the exit of the magnet (true thickness), and the following detectors with their true thicknesses, SFD-x and SFD-w planes, one plane of the MSGC and one plane of IH. Each scatterer was 100 mm wide and 25 mm high. They were placed in the negative arm of the spectrometer, after the drift chamber DC3 (c.f. figure 1), in a vertical ladder (c.f. figure 2) with empty space (control region A) between the scatterers. Remark that DIRAC-ms does not exist for the IH, and Moliere-ms was used instead for Monte Carlo simulations.

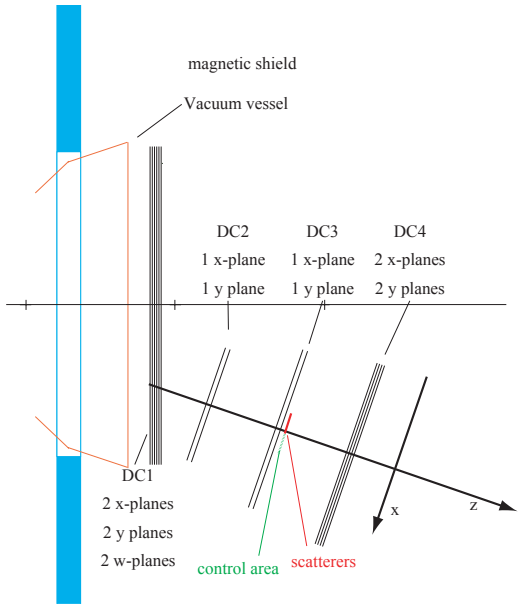

Figure 1: *Set-up for the measurement of multiple scattering in various scatterers.*

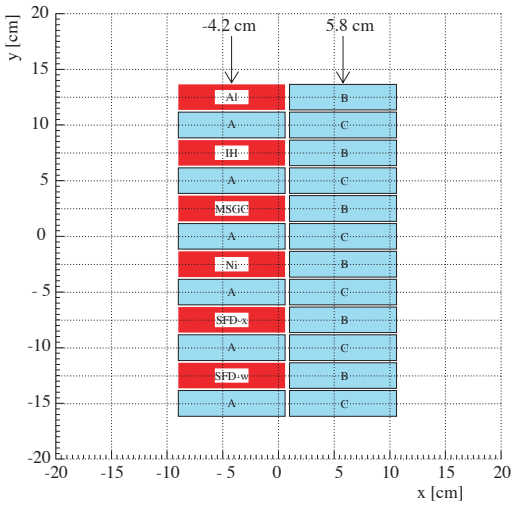

Figure 2: *The position of the scatterers (solid boxes - SFD-w, SFD-x, Ni, MGSC, IH, Al) and control regions - A, B and C.*

All scatterers were put at the same x-position of -4.2 cm (x_{center}) in the coordinate system of the negative arm of the spectrometer, and the y-gap between them was 2.5 cm. The distance between the scatterers and the last plane of DC3 (4-y-r) was 26 mm.

In order to avoid any boundary effects, only pion tracks were accepted which passed the smaller size box 96×22 mm^2. The momentum acceptance is shown in Fig. 3.

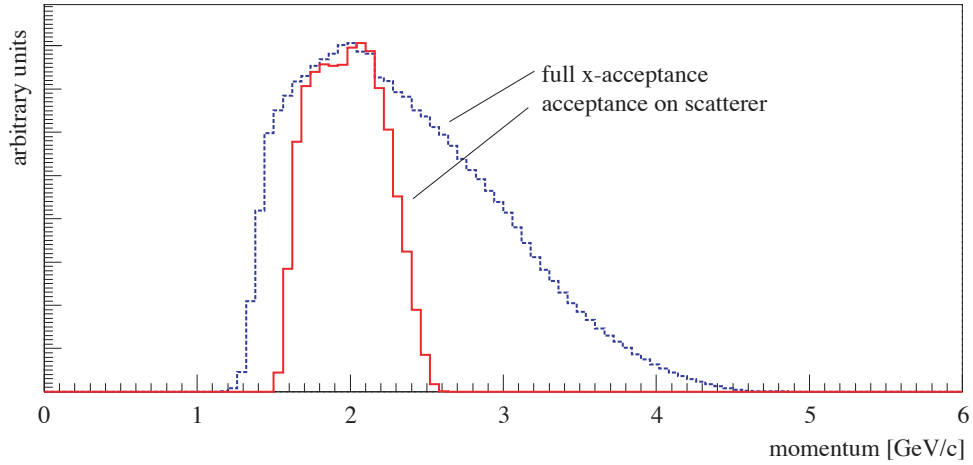

Figure 3: *The pion momentum distributions for scatterers and for all the tracks.*

For the sake of completeness we recall the standard formula for multiple scattering [1]:

$$\alpha_0 = \frac{0.0136[GeV/c]}{\beta P}\sqrt{\frac{x}{X_0}} \tag{1}$$

with α_0 the projected rms scattering angle, $\beta \approx 1$ and P (GeV/c) the velocity and momentum, respectively of the particle, X_0 the radiation length and x the thickness of the scatterer.

Three different methods were used in order to extract results:

- **Method 1:**Tracks (straight lines) were reconstructed using the six planes from DC1, the two planes from DC2 and two planes from DC3. The tracks were extrapolated to the scatterer plane and then to DC4. At DC4 the difference Δ between the extrapolated and the real hit coordinates ($\Delta x = x_{hit} - x_{extrapolated}$, analogously for y) was determined and the angular deflections $\alpha_x(\alpha_y)$ between incoming and scattered tracks were deduced. The momentum independent quantities $\delta_{x,y} = \alpha_{x,y} * P/0.0136$ (square root of thickness in units of radiation length, see Eq. 1) were then used for comparisons between experimental values and simulated ones.

- **Method 2:** Tracks were reconstructed as above for the x-coordinate only, and distributions for the scatterers and the control regions A were obtained. The distributions from control region A were then folded analytically with the multiple scattering algorithms mentioned above (DIRAC-ms and Moliere-ms) and compared with the measured experimental scattering distribution. A least squares method was applied to fit the folded distribution to the experimantal scattering distribution by varying the sigmas of the multiple scattering distribution (DIRAC-ms and Moliere-ms).

- **Method 3:** No track fit was done but the hit coordinates in DC2 and DC3 were used to calculate the track parameters of the incoming track and to extrapolate it to the scattering plane and to DC4. The track coordinates at the scattering plane and the real hits in DC4 determined the scattered track. The deflection angle was obtained from the scalar product of the track's unit vectors, and the quantities δ_x and δ_y were obtained for experimental data and simulated ones.

2 Results from Method 1.

Tracks which pass through our special scatterers were selected by applying cuts on x- and y-coordinates of tracks in the scatterer plane: $|x - x_{center}| < 4.8cm$ and $|y - y_{center}| < 1.1cm$, where x_{center} and y_{center} are the coordinates of scatterer centers. For each scatterer region we obtained the distributions of δ_x and δ_y whose central parts were fitted by Gaussians, resulting in sigmas and mean values and their corresponding errors.

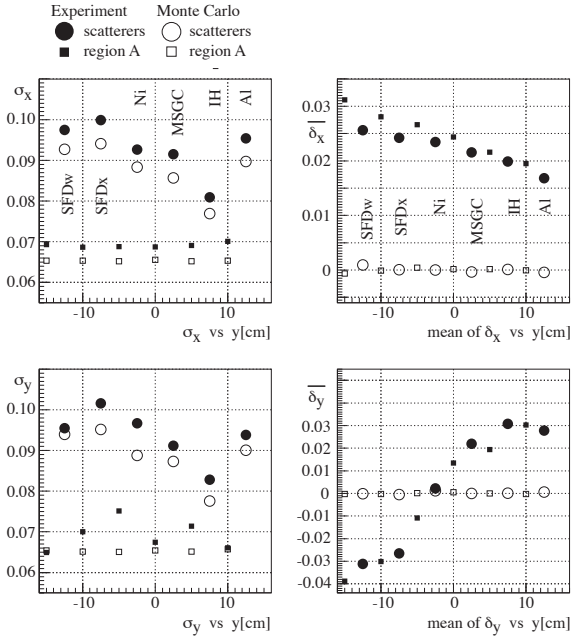

Figure 4: *σ_x and σ_y of the distributions of δ_x, δ_y, and their mean values $\overline{\delta_x}$, $\overline{\delta_y}$, for experimental (black marks) and Monte-Carlo (empty marks) data for scatterers (circles) and for control regions A(squares).*

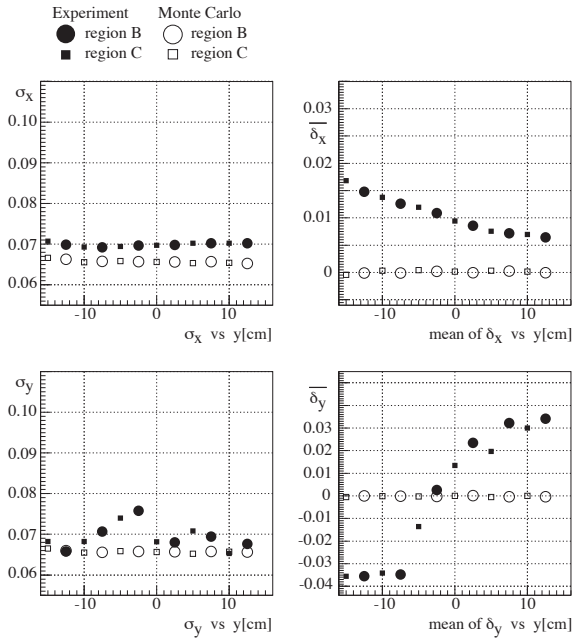

Figure 5: *Same as Figure 4, but for control regions B and C.*

Figure 4 shows the $\sigma_x(\sigma_y)$ and mean values $\overline{\delta_x}(\overline{\delta_y})$ for experimental and the DIRAC-ms Monte-Carlo data for the scatterers and for the control regions A.

The following may be observed:

- the measured values of σ_x and σ_y are larger than the simulated ones, both for the scatterers and for the control regions A.
- The mean values $\overline{\delta_x}(\overline{\delta_y})$ are zero for Monte Carlo data, while the measured ones show significant systematic offsets, which are the same for scatterers and for control region A.

– in x-direction the maximum offset (0.03) is obtained for the lowest (negative) y-value, the smallest one (0.016) for the highest (positive) y-value. The offset is roughly linear ($\overline{\delta_x} = 0.025 - 4 \times 10^{-4} \times y[cm]$).

– in y-direction the offsets change sign and vary smoothely from -0.04 to 0.03, thus span a range of 0.07. A linear 1st order approximation follows roughly $\overline{\delta_y} = 0.0033 + 3 \times 10^{-3} \times y$ [cm].

The control regions regions B and C were studied in a similar way. The results are shown in Fig.5. No differences are observed between regions B and C. The offsets in x-direction follow the same slope as for the scatterers and regions A, but are lower by 0.01, whereas the offsets in y-direction are essentially the same.

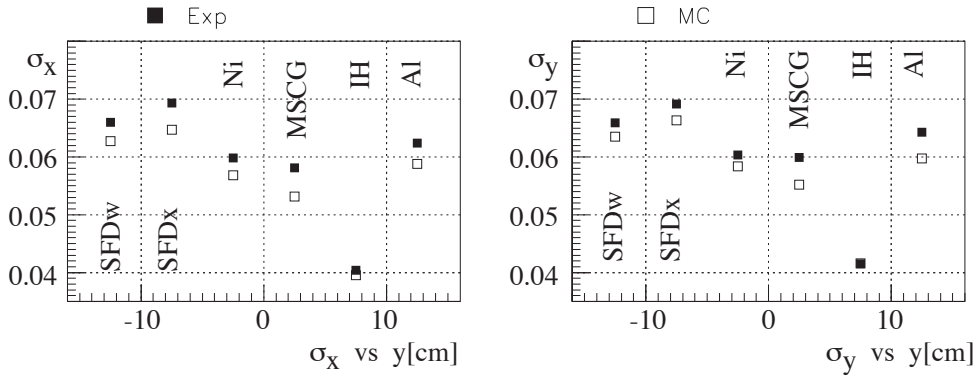

Figure 6: *Reduced sigmas,* $\sigma_x = \sqrt{\sigma^2_{x,scatt} - \sigma^2_{x,A}}$ *and* $\sigma_y = \sqrt{\sigma^2_{y,scatt} - \sigma^2_{y,A}}$ *for all scatterers and full momentum acceptance.*

The observed offsets of the distributions for the different scatterers and control regions may possibly be due to either additional (toroidal) magnetic fields, or by improper alignment to be remedied by appropriate rotations, e.g. of the planes of DC2.

Multiple scattering caused by the scatterers alone may be isolated through the reduced sigmas $\sqrt{\sigma^2_{x,scatt} - \sigma^2_{x,A}}$ (analogously for y). In Fig.6 we present the reduced sigmas for all accepted momenta, as measured and from DIRAC-ms Monte Carlo. We observe that experimental values are systematically larger than the DIRAC-ms simulation ones, except for the IH, where Moliere-ms was used.

In Fig.7 we compare the reduced sigmas from simulations for Moliere-ms and for DIRAC-ms. We observe the following:

- for Ni, Al and IH, which are unambigously described in the detector descriptions
  - experimental values and Moliere-ms coincide.
  - differences between Moliere-ms and DIRAC-ms are the same for Al and Ni, namely of 5.1 % in the average of x and y, Moliere-ms providing the larger values.
- the differences Moliere-ms minus DIRAC-ms for the other scatterers are as follows:
  - MSGC; -4.5%
  - SFDx: -1.0 %

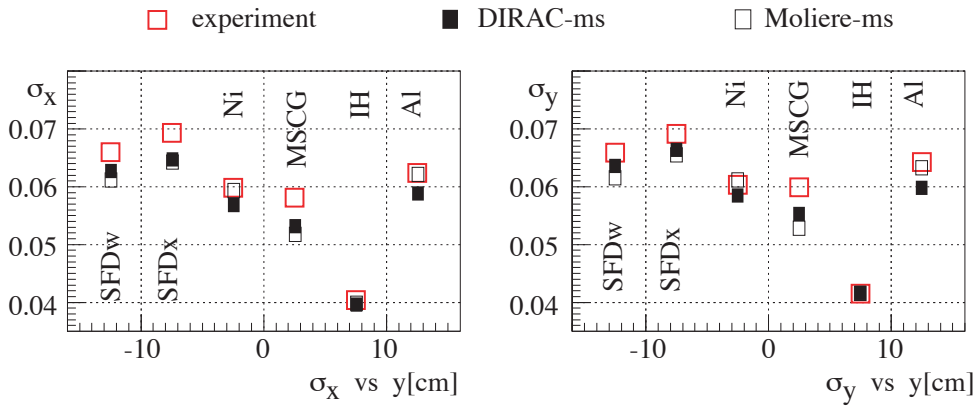

Figure 7: *Reduced sigmas from Monte Carlo simulations, using Moliere-ms, and DIRAC-ms. For comparison we also show the experimental reduced sigmas from Fig. 6.*

– SFDw: -2.9 %.

From Al, Ni and IH we conclude, that Moliere-ms describes the experiment well, and that DIRAC-ms is about 5% to narrow. From this observation we may further conclude that the other detectors require the following corrections in order to make Moliere-ms simulations coincide with the experimental reduced sigmas:

- MSGC; sigma: 11.2%, effective thickness: 24%.
- SFDx: sigma: 6.1%, effective thickness: 13%.
- SFDw: sigma, 6.6%, effective thickness: 14%.

The corrections suggest that the SFDw and SFDx are well described by the detectror description in DIRAC-GEANT, provided their thickness is enlarged by 13.5% for both. The effective thicknesses of the MSGC in the detector description has to be increased by 24% in order to describe the scattering measurement properly with Moliere-ms.

3 Results from Method 2.

Description of the method and definitions: The10 planes from DC1, DC2 and DC3 (from 1-x-r to 4-y-r) were used. Only tracks were accepted where all planes had proper hits, and drift distances were in the range $0.02 < d < 0.48$ cm in order to exclude particles that passed to close to the wires. The track was propagated to the level of 5-x-r plane of DC4 and hits were searched for in the range ± 0.2 cm around the predicted point. Only one hit is allowed. Additionally, only hits were selected with drift distance larger than 0.2 cm. This criterion reduces the probability of wrong hit identification due to left-right ambiguity. For a selected track the angle of deflection in x-direction was calculated according to:

$$\alpha_x = \frac{\arctan(A_x + \frac{\Delta x}{\Delta z\sqrt{1+A_y^2}}) - \arctan A_x}{(1 + A_x^2 + A_y^2)^{1/4}}$$

Here, A_x and A_y are x- and y-components of the track direction vector ($A_z = 1$), Δx is the difference between measured and predicted coordinates at the 5-x-r plane, Δz is the difference in z-coordinate between the scatterer plane and the 5-x-r plane of DC4. The factor $(1 + A_x^2 + A_y^2)^{1/2}$ in the denominator corrects the effective thickness for tracks which are not normal to the scatterer surface to the thickness of the scatterer [1].

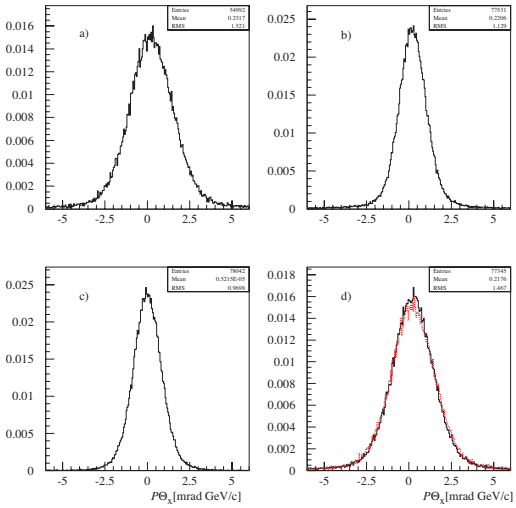

Figure 8: *Distribution $P\alpha_x$ for: (a) experimental tracks through the Ni scatterer, (b) experimental tracks through surrounding control regions A, (c) multiple scattering in the Ni scatterer simulated with DIRAC-ms, (d) folded ("mixed") distribution (solid line) and distribution (a) (dashed line) for comparison. All distributions are normalized to unity.*

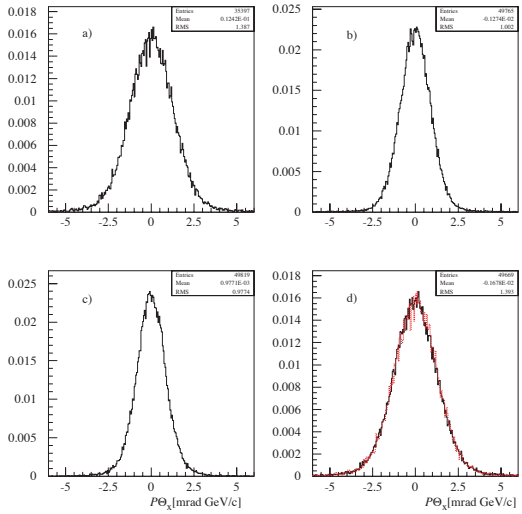

Figure 9: *Distribution $P\alpha_x$ for: (a) Monte Carlo simulated tracks through the Ni scatterer, (b) Monte Carlo simulated tracks through the surrounding regions A, (c) multiple scattering in the Ni scatterer simulated with DIRAC-ms, (d) folded ("mixed") distribution (solid line) and distribution (a) (dashed line) for comparison. All distributions normalized to unity.*

Results for Ni: In Fig. 8a, the distribution over angle of deflection α_x multiplied by the particle laboratory momentum P is shown for tracks which crossed the Ni scatterer. In Fig. 8b, the analogous distribution is shown for tracks having passed the surrounding control regions A (above and below the scatterer). Comparison shows the additional scattering in the Ni scatterer. Fig. 8c shows the distribution of multiple scattering angles for Ni simulated with DIRAC-ms. The simulation is based on the DIRAC-ms analytic algorithm and the measured momenta. Folding of the simulated distribution with the distribution of the control regions A results in the "mixed" distribution and is presented in Fig. 8d. It is expected to represent the measured distribution for tracks that crossed the Ni scatterer (Fig. 8a), shown also by the dashed line. A small discrepancy is evident.

For comparison the same distributions for Monte Carlo simulated events are shown in Fig. 9b. In this case the agreement is good and proves that the folding method works.

Correction method for Ni: In order to pin down the discrepancy between "measured" multiple scattering and the DIRAC-ms multiple scattering algorithm, the angles obtained with

[1] it should be noted that the following results were obtained with the denominator $(1 + A\,\frac{2}{x} + A_y^2)^{1/2}$ instead of $(1 + A_x^2 + A_y^2)^{1/4}$.

DIRAC-ms algorithm or the standard Moliere multiple scattering formula have been multiplied by a factor $\kappa \in [0.7, 1.3]$ and were used to construct simulated distributions of the type Fig. 8c. These distributions were folded with the measured distributions for tracks from the surrounding regions A and resulted in "mixed" distributions. The "mixed" distributions for each κ were used to determine the optimum κ by comparing them with the measured scattering distribution Fig. 8a using the over-all χ^2. The χ^2 values as function of κ are shown for experimental data and DIRAC-ms multiple scattering (Fig. 10a), for experimental data and Moliere-ms description (Fig. 10b), for Monte Carlo simulated data and DIRAC-ms description (Fig. 10c). Minimum χ^2 is achieved at $\kappa = 1.08$ (Fig. 10a). The "mixed" distribution for this value is shown in Fig. 10d (dashed line) in comparison with the experimental distribution for Ni (solid line). Agreement seems to be better than in Fig. 8d.

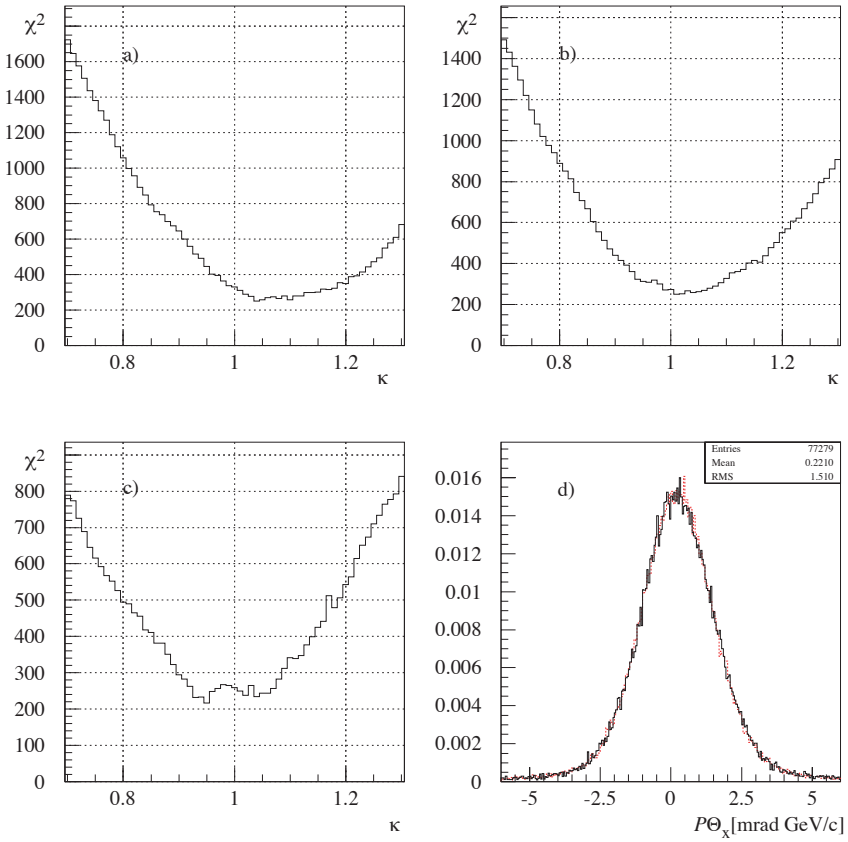

Figure 10: *χ^2 as a function of κ for tracks scattered in Ni for: (a) experimental data and DIRAC-ms description of multiple scattering, (b) experimental data and Moliere-ms description, (c) Monte Carlo simulated data and DIRAC-ms description. (d) Dashed line shows "mixed" distribution with DIRAC-ms multiple scattering for $\kappa = 1.08$, the solid line shows experimental distribution of tracks through the Ni scatterer.*

Corrections for all scatterers and conclusions: This procedure was applied for all scatterers, and κ values for χ^2 minima are presented in Table 1. The accuracy is ~ 0.01. Two fit ranges in $P\alpha_x$ were used. The results are quite insensitive to the fit range.

Independent of the scatterer, the DIRAC-ms description needs in the average a factor $\kappa = 1.08$ in order to describe the experimental distribution. This leeds to the conclusion that the angle in DIRAC-ms is in general underestimated by 8%. This may reflect the fact, that in [2]

the shape of the distributions (sigmas) and the effective thickness were mixed up through the algorithm.

The Moliere-ms description makes use of the GEANT detector description. The factors for Al, Ni, and SFDw are very similar and ~ 1.03. This does not necessarily mean that the angle is underestimated by 3% but rather reflects the incorrect thickness correction. The description is poor for the MSGC (1.12) and for SFDx (1.20). From the numbers we conclude that, if Moliere-ms is assumed to be correct, the effective thickness of the Al and Ni scatterers remain unchanged (thickness correction), SFDw has to be increased by 6%, the one for MSGC by 26 % and the one for SFDx by 46%.

Table 1: Coefficient κ for minimum χ^2 in comparing "mixed" and experimental distributions of tracks crossing the scatterers

	Range ± 4 mrad·GeV/c		Range ± 6 mrad·GeV/c	
	DIRAC-ms	Moliere-ms	DIRAC-ms	Moliere-ms
Al	1.075	1.040	1.068	1.033
MSGC	1.077	1.124	1.080	1.123
Ni	1.078	1.028	1.081	1.025
SFDx	1.099	1.211	1.095	1.205
SFDw	1.088	1.046	1.082	1.035

4 Results from Method 3.

Definitions are as in section 2. The track hit candidates in all drift chamber planes were obtained by releasing the χ^2 conditions in the initial momentum determination. This should eliminate possible biases in DC4 for large scattering angles by the scatterers. This reconstruction leads to tails of the $\delta_{x,y}$-distributions. Typical shapes are shown in Fig 11. We observe that the reconstruction produces tails for experimental data, which are not reproduced by the simulations. The stronger cuts as well as the fits including DC1 as used in Method 1 and Method 2 do not show these tails. We conclude that strong cuts may produce biases.

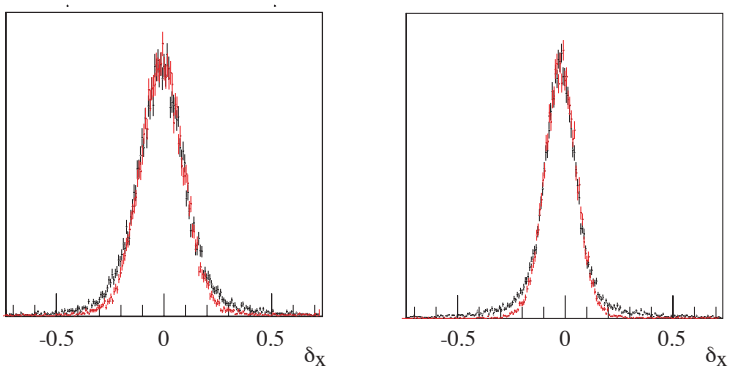

Figure 11: *Shapes of the distributions in δ_x, left for the Ni scatterer (experimental data black, Moliere-ms simulation red), right for the corresponding control region. Method 3.*

For determining the width and the mean values of the $\delta_{x,y}$ distributions, Gaussians were fitted to the distributions. The tails for the experimental distributions were accounted for by a second Gaussian with larger width. Values retained are from the narrower Gaussian.

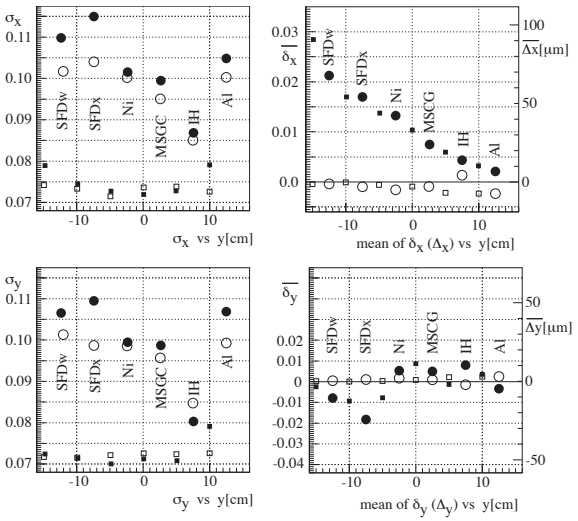

Figure 12: σ_x and σ_y and mean values $\overline{\delta_x}$, $\overline{\delta_y}$ of the distributions of δ_x, δ_y, and their mean values , for experimental (black marks) and Monte-Carlo DIRAC-ms (empty marks) data for scatterers (circles) and for control regions A(squares). For comparison the mean values $\overline{\Delta_x, y}$ are also given for the spatial distributions δ_x, y at DC4. Method 3.

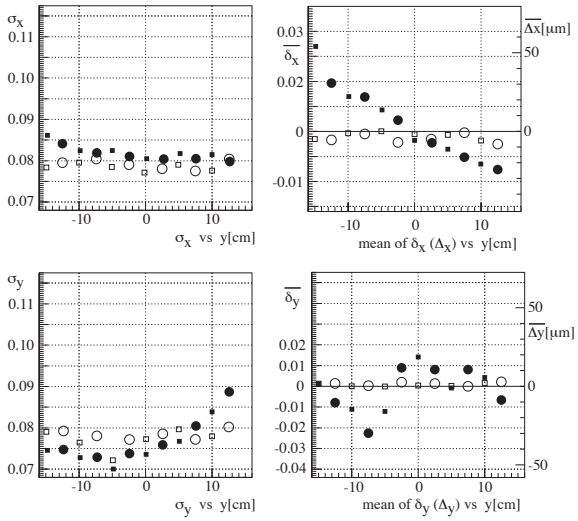

Figure 13: *σ_x and σ_y and mean values $\overline{\delta_x}$, $\overline{\delta_y}$ of the distributions of δ_x, δ_y, and their mean values, for experimental (black marks) and Monte-Carlo DIRAC-ms (empty marks) data for control regions B (circles) and C (squares). For comparison the mean values $\overline{\Delta_x, y}$ are also given for the spatial distributions δ_x, y at DC4. Method 3.*

Figures 12 show the sigmas and the offsets of the distributions $\delta_{x,y}$, for scatterers and control regions A from experimental data and from simulations with DIRAC-ms. Fig. 13 shows the same for control regions B and C.

The offsets (mean values) in x and y show the following behaviour:

- in x-direction the offsets for experimental data show a strong dependence on the vertical position y. It may roughly be described as $\overline{\delta_x} = +0.011 - 8.5 \times 10^{-4} \times y$
- in x-direction the offset is zero for Monte Carlo
- in y-direction the offsets for experimental data are almost zero. A first order linear approximation is roughly following $\overline{\delta_y} = 0 + 5 \times 10^{-4} \times y$.
- in y-direction the offsets are zero for Monte Carlo.
- for control regions B and C the offsets show the same features as for the scatterers, except that in x-direction there is a constant shift downwards of 0.01.

For comparison the mean values in Figures 12,13 are also given for the spatial distributions at DC4. We remind that the spatial resolution of a drift chamber is about 80 μm. The offsets are equal or smaller than the resolution, but systematic.

Comparing this with the findings of Method 1, we observe, that

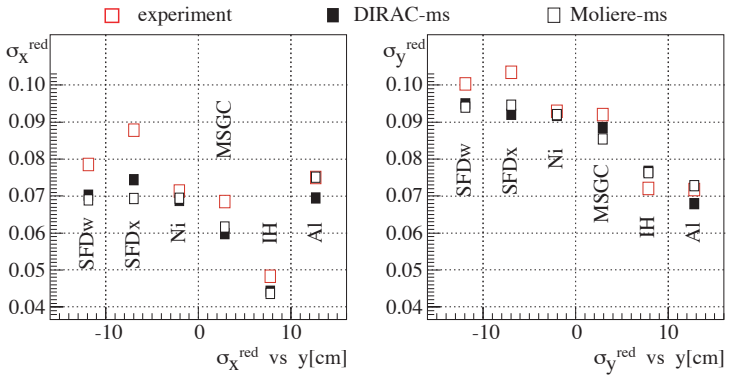

Figure 14: *Reduced sigmas of the $\delta_{x,y}$-distributions for experimental data and simulations. Method 3.*

- in x-direction the offsets for experimental data have changed from a slope of 4×10^{-4} to 8.5×10^{-4}, leading to the conclusion that the track fitting in Method 1 has smoothed away a possible misalignment.
- in y-direction the offsets for experimental data have almost disappeared, indicating, that the effect in y seen in method 1 might be due to an additional magnetic field, which is strong in DC1 and absent in DC2.

The reduced sigmas were obtained as described in Section 2. They are shown in Fig. 14. We observe

- that the reduced sigmas in x and y direction are quite different,
- that the experimental points are larger than the simulated ones.
- agreement between Moliere-ms and experimental data for Ni and Al (averaged differences of +2% and 1%, respectively for Moliere-ms, -6% and -2% for DIRAC-ms).
- a difference, averaged over x and y, of -9% (MSGC), -15% (SFDx) and -9% (SFDw) for Moliere-ms, and of -8% (MSGC), -13% (SFDx) and -8% (SFDw) for DIRAC-ms.

These findings confirm the earlier conclusion, that Moliere-ms reproduces experimental data well for Al and Ni, where the material budget is well known. DIRAC-ms in general has adapted the algorithms to the measurement. The study also confirms that the effective thickness of the MSGC is underestimated in the DIRAC-GEANT detector description (about 17%). Sizable effects are also found for the SFDs.

We would, however, stress, that the method is not optimally suited for widths determinations, due to the pronounced sensitivity to alignment.

5 Summary

The study of multiple scattering using the special scattering data from 2003 and standard ARIANE procedures was done in three independent and different ways (Methods 1, 2 and 3). All three methods have shown the following:

- DIRAC-ms provides too narrow distributions.
- Moliere-ms describes the measured data well for materials with well defined material budgets (Al, Ni).

- The material budget for MSGC and SFD as tabulated in the DIRAC GEANT detector description is wrong. This analysis provides a direct measurement of the real thickness of these detectors. Method 1 provides the following increases of effective thickness with respect to the actual detector description values:
  - MSGC: 24%
  - SFDx,y,w: 13.5%
- Method 1 and 3 show serious deficiencies in comparing the mean values (offsets) of the distributions $\delta_{x,y}$ and $\Delta_{x,y}$ when compared to Monte Carlo simulation. There are strong dependences of these mean values from the vertical position of the investigated regions. These dependences are different in appearence for x- and y-direction.
- These offsets may be due to misalignment or magnetic fields.
- Method 3 showed that in x-direction the offsets are most likely due to misalignment, while in y-direction magnetic fields may be responsible.

The need for larger multiple scattering was recognized already by Schuetz [3] and, more recently, by Adeva et al. [4].

While the results on multiple scattering will lead to the appropriate algorithms and detector descriptions, the problem of alignment/magnetic fields needs further studies and corrections. Although the offsets are smaller than the spatial resolution of the drift chambers, they show a systematic behaviour and may thus lead to observable deteriorations in momentum reconstruction.

References

[1] Particle data group, Physics Lett. B592 (2004) 1

[2] A. Dudarev, V. Kruglov, L. Kruglova, M. Nikitin [JINR], DIRAC Note 2005-02.

[3] Christian Schuetz, University of Basel, 26 March 2004 2002.

[4] Adeva et al, DIRAC NOTE 05-16